A Metamaterial-Based Multiband Phase Shifter

Michael Maassel, Benjamin D. Braaten, and David A. Rogers
Electrical and Computer Engineering
North Dakota State University
Fargo, North Dakota 58102
Email: michael.maassel@ndsu.edu

***Abstract*—A design methodology for a multi-band phase shifter using a metamaterial-based transmission line was developed. This method is different in that the loaded-line phase shifter has a phase shift of 90 ° at the center frequencies of both bands (ISM bands: 902 - 928 MHz and 2400 - 2498 MHz) instead of -90 ° and -270 °. The method was validated using simulation and measured results.**

I. Introduction

Phase shifters are used in several different microwave and RF applications, including phased-array antennas, radar systems, and phase-noise measurement systems. The current research on metamaterial-based phase shifters is very limited. The research relies on simulations to provide the values for the metamaterial portion of the phase shifter, a method that can be prone to errors. The methodology developed here provides analytically computed values for the metamaterial transmission line before the circuit is simulated. These values were validated with both simulation and measured results.

A. An Introduction to Metamaterials

Metamaterials are artificial media with properties not readily available in nature. Examples of metamaterials include electromagnetic band gaps, artificial magnetic conductors, and double-negative or left-handed materials [1]. Double-negative or left-handed materials have both a negative permittivity and permeability, giving a negative phase velocity.

The left-handed transmission line was fabricated using lumped-element components (series capacitors and shunt inductors). With the parasitic nature of these components, a pure left-handed transmission line cannot be realized. Instead the line is a combination right/left-handed (CRLH) transmission line. At low frequencies the CRLH transmission line will function as a left-handed line and at high frequencies it will function as a right-handed line.

The design equations for a left-handed transmission line are developed by analyzing an infinite periodic transmission line with series and parallel loads as shown in Fig. 1 [2].

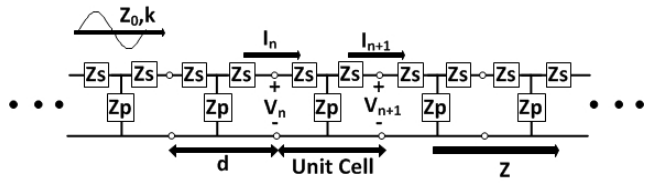

Fig. 1. Generalized Infinite Periodic Transmission Line with Series and Parallel Loads.

B. Loaded Line Phase Shifter

The loaded-line phase shifter (Fig. 2) was selected since it can have a broad range of phase shifts and the phase shifts are not confined to set values.

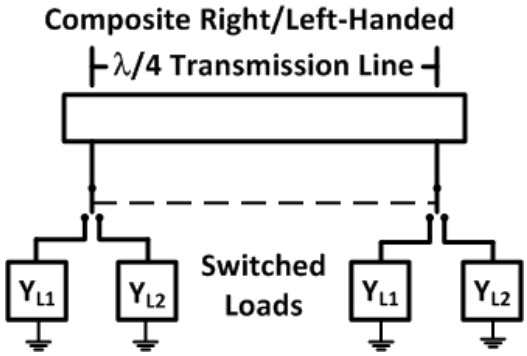

Fig. 2. Loaded-Line Phase Shifter.

Step 1: Determine the desired phase shift at each frequency f_1 = 915 MHz and f_2 = 2450 MHz is

$$\phi(f_1) = 90\,^\circ \tag{1}$$

and

$$\phi(f_2) = 90\,^\circ. \tag{2}$$

The total phase shift is equal to the sum of the phase shift from the right-handed and left-handed transmission lines, or

$$\phi_c = \phi_R + \phi_L, \tag{3}$$

and

$$\frac{\pi}{2} = -2\pi f N\sqrt{L_R C_R} + \frac{N}{2\pi f}\frac{1}{\sqrt{L_L C_L}} \tag{4}$$

where N is the number of sections in the CRLH transmission line. Setting

$$P = -2\pi N\sqrt{L_R C_R} \tag{5}$$

and

$$Q = \frac{N}{2\pi}\frac{1}{\sqrt{L_L C_L}}, \tag{6}$$

the values for P and Q are calculated, and the results are: $P = 4.6680 \times 10^{-10}$ s and $Q = 1.0465 \times 10^{9}\,\frac{1}{\mathrm{s}}$.

Step 2: Choose a value for N in the equation. ϕ_L is the unit cell phase shift. N is arbitrarily chosen as 5; therefore,

$$\phi_L = \frac{TotalPhaseShift}{2 \times N} = \frac{180}{10} = 18^\circ. \tag{7}$$

978-1-4799-4774-4/14/$31.00 ©2014 IEEE

Step 3: Use the Q and N values to determine the L_L and C_L product. Thus,

$$Q = \frac{N}{2\pi}\left(\frac{1}{\sqrt{L_L C_L}}\right) \tag{8}$$

and

$$L_L C_L = \left(\frac{N}{2\pi Q}\right)^2. \tag{9}$$

The result is:

$$L_L C_L = 9.2524 \times 10^{-20}\ s^2 \tag{10}$$

Step 4: Solve for L_L and C_L with the $L_L C_L$ product and the selected characteristic impedance $Z_{0L} = 50\ \Omega$ yields:

$$L_L = 1.5209 \times 10^{-08} = 15\ \text{nH} \tag{11}$$

and

$$C_L = 6.0836 \times 10^{-12} = 6\ \text{pF}. \tag{12}$$

Step 5: Use Pf_1 or Pf_2 to obtain the electrical length of the right-handed transmission line (RHTL). P was defined in (5) and f_1 and f_2 are the center frequencies of the two bands of interest (915 MHz and 2450 MHz). Electrical length is defined as the length of a transmission medium expressed as the number of wavelengths of the signal propagating in the medium. Note that the electrical length is in general different from the physical length.

The electrical length was calculated to be 24.5°. With the electrical length determined, the length and width of the right-handed transmission line is calculated. Linecalc, from ADS, was used to determine these values. The material parameters were obtained from the data sheet of the printed circuit board (pcb) material that was selected for this project (Rogers RO4003C) as shown in Table I. Linecalc gave the results for the two transmission lines in Table II.

TABLE I. PRINTED CIRCUIT BOARD DATA USED IN LINECALC.

Substrate Dielectric Constant (ϵ_r	3.38
Substrate Thickness (H)	0.813 mm
Loss Tangent (TanD)	0.0021
Copper Thickness (T)	0.0356 mm
Impedance	50 Ω
Trace Length	Set at 24.5° as a starting point

TABLE II. PHYSICAL PARAMETERS FOR THE TRANSMISSION LINES.

	Microstrip	Coplanar Waveguide with Ground (CPWG)
Line Width	1.78 mm	1.77 mm
Line Length	13.4 mm	13 mm
Gap	-	1 mm

The line impedance and capacitance values for the different phase shifts were calculated at the two center frequencies (f_1 = 915 MHz and f_2 = 2450 MHz) using (13) through (17). The phase shift values went from 10° to 45° in 5° steps. The impedance and electrical length of the transmission line was set at 50 Ω and 90°. The admittance of the transmission line with a phase shift is given by

$$Y_C = Y_0 \sec\left[\frac{phaseshift}{2}\right]\sin\beta l, \tag{13}$$

and the shunt admittance is

$$B_{L1} = Y_0 \cos(\beta l)\sec\left[\frac{phaseshift}{2}\right] + \tan\left[\frac{phaseshift}{2}\right]. \tag{14}$$

The reactance of the phase shift capacitance is

$$X_{L1} = \frac{1}{B_{L1}}. \tag{15}$$

The capacitance values at the two center frequencies are

$$C_1 = \frac{1}{2\pi f_1 X_{L1}}, \tag{16}$$

and

$$C_2 = \frac{1}{2\pi f_2 X_{L1}}. \tag{17}$$

The results are listed in Tables III and IV.

TABLE III. CAPACITANCE VALUES FOR DIFFERENT PHASE SHIFTS AT 915 MHZ.

Phase Shift	10 °	15 °	20 °	25 °	30 °	35 °	40 °	45 °
C1 (pF)	0.304	0.458	0.613	0.771	0.932	1.097	1.266	1.441

TABLE IV. CAPACITANCE VALUES FOR DIFFERENT PHASE SHIFTS AT 2450 MHZ.

Phase Shift	10 °	15 °	20 °	25 °	30 °	35 °	40 °	45 °
C2 (pF)	0.114	0.171	0.229	0.288	0.348	0.410	0.473	0.538

C. Simulation

The simulation software that was used is Agilent's Advanced Design System (ADS). Specifically, the linear component simulation engine and the 2.5-D electromagnetic simulation engine were used. Murata Electronic capacitor and inductor models were used for the lumped components and Infinion S-Paramater files were used for the varactor diodes at various bias voltages.

The simulation schematic is shown in Fig. 3. The simulation results for phase shift, insertion loss and return loss for different values of bias voltages are shown in Tables V and VI.

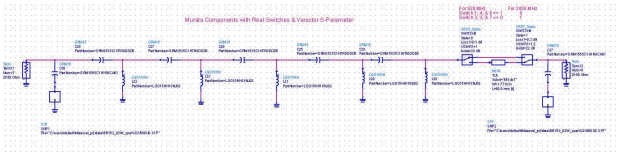

Fig. 3. Simulation Schematic with Murata Components and S-Parameter Files for the Varactor Diodes.

D. Testing and Results

The board (Fig. 4) was connected to the network analyzer and DC bias was applied. The phase shift for each bias voltage is shown in Table VII. The insertion loss and return loss for each bias voltages is shown in Table VIII.

TABLE V. SIMULATION RESULTS SHOWING THE PHASE SHIFT, INSERTION, AND RETURN LOSS FOR DIFFERENT VALUES OF VARACTOR BIAS VOLTAGES AT 920 MHZ.

920-MHz Output			
Bias Voltage	Phase Shift	Insertion Loss	Return Loss
0.5 V	5.4°	1.67 dB	9.97 dB
0.6 V	5.6°	1.66 dB	10 dB
0.7 V	5.7°	1.65 dB	10.1 dB
0.8 V	5.8°	1.65 dB	10.1 dB
0.9 V	5.9°	1.65 dB	10.1 dB
1.0 V	6°	1.64 dB	10.2 dB
1.5 V	6.5°	1.62 dB	10.3 dB
2.5 V	7.3°	1.6 dB	10.6 dB
3 V	7.6°	1.6 dB	10.7 dB
3.5 V	7.96°	1.56 dB	10.8 dB
4 V	8.29°	1.6 dB	10.9 dB
4.5 V	8.6°	1.54 dB	11 dB
5 V	8.96°	1.53 dB	11.1 dB
6 V	9.6°	1.5 dB	11.4 dB
7 V	10.1°	1.49 dB	11.5 dB

TABLE VI. SIMULATION RESULTS SHOWING THE PHASE SHIFT, INSERTION, AND RETURN LOSS FOR DIFFERENT VALUES OF VARACTOR BIAS VOLTAGES AT 2450 MHZ.

2450-MHz Output			
Bias Voltage	Phase Shift	Insertion Loss	Return Loss
0.5 V	-15.6°	2.5 dB	4.2 dB
0.6 V	-15.3°	2.5 dB	4.3 dB
0.7 V	-14.9°	2.4 dB	4.3 dB
0.8 V	-14.6°	2.4 dB	4.4 dB
0.9 V	-14.3°	2.37 dB	4.4 dB
1.0 V	-14°	2.34 dB	4.5 dB
1.5 V	-12.7°	2.19 dB	4.7 dB
2.5 V	-10.4°	1.95 dB	5.2 dB
3 V	-9.4°	1.85 dB	5.4 dB
3.5 V	-8.5°	1.75 dB	5.6 dB
4 V	-7.5°	1.67 dB	5.8 dB
4.5 V	-6.6°	1.58 dB	6 dB
5 V	-5.6°	1.5 dB	6.2 dB
6 V	-3.6°	1.34 dB	6.7 dB
7 V	-2.4°	1.24 dB	7 dB

TABLE VII. MEASURED PHASE SHIFT VALUES FOR DIFFERENT VARACTOR BIAS VOLTAGES WITH A 10-PF CAPACITOR IN SERIES WITH THE VARACTOR AT 920 AND 2450 MHZ.

Bias Voltage	S_{21} Phase at 920 MHz	S_{21} Phase at 2450 MHz
0	-51	65
0.1	-50.8	53.7
0.2	-49	36
0.3	-47.7	18
0.4	-45.6	1.6
0.5	-44	-10.8
0.6	-43.6	-25.8
0.7	-43	-70
0.8	-42	-90
0.9	-41.5	-107
1	-41	-133
1.5	-38	-148
2	-35	-143
2.5	-34	-133
3	-32	-119
4	-29	-88
5	-26	-63
6	-25	-53
7	-25	-50

II. CONCLUSION

The performance of the phase shifter was good to excellent. The design procedure is easy to follow and the results are close to the optimized component values that were obtained from the simulation program.

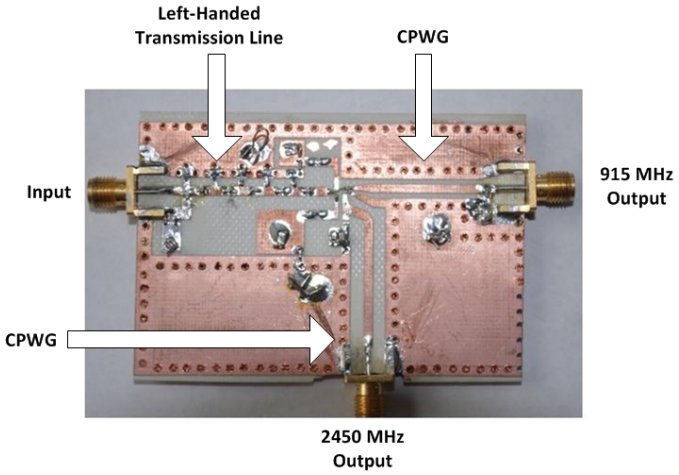

Fig. 4. Assembled Printed Circuit Board.

TABLE VIII. MEASURED INSERTION AND RETURN LOSS FOR DIFFERENT VARACTOR BIAS VOLTAGE WITH A 10-PF CAPACITOR IN SERIES WITH THE VARACTOR AT 920 AND 2450 MHZ.

Bias Voltage	Insertion Loss at 920 MHz	Return Loss at 920 MHz	Insertion Loss at 2450 MHz	Return Loss at 2450 MHz
0	0.44	22	2	8
0.1	0.35	28	1.6	8
0.2	0.35	26	1.6	8
0.3	0.35	25	1.6	8
0.4	0.33	32	1.5	8
0.5	0.4	30	1.6	8
0.6	0.49	28	1.5	7
0.7	0.45	28	1.8	8
0.8	0.47	29	1.8	7
0.9	0.45	28	1.8	7
1	0.44	28	1.8	7
1.5	0.44	29	1.8	7
2	0.45	25	1.8	7
2.5	0.45	25	1.8	7
3	0.45	25	1.8	7
4	0.45	25	1.8	7
5	0.45	25	1.8	7
6	0.45	25	1.8	7
7	0.45	25	1.8	7

ACKNOWLEDGMENT

The authors would like to acknowledge the help and support of the following faulty members in the development of this work: Dr. Robert Nelson, University of Wisconsin-Stout and Drs. Orven F. Swenson and Subbaraya Yuvarajan, North Dakota State University.

REFERENCES

[1] Arnab Bhattacharya (2013, September 26). "Modeling and Simulation of Metamaterial-Based Devices for Industrial Applications Webinar," *Computer Simulation Technology*, Available: http://www.cst.com

[2] B. Braaten and R. Scheeler, *"Radio Frequency Identification Fundamentals and Applications, Design Methods and Solutions,"* Intech, February, 2010, Chapter 4.